Hindawi
Journal of Nanomaterials
Volume 2022, Article ID 9958031, 12 pages
https://doi.org/10.1155/2022/9958031

Research Article

Preparation and Characterization of Ultra-Fine 3-Nitro-1,2,4-Triazole-5-One Crystals Using a Novel Ultrasonic–Assisted Spray Technology

Huimin Liu, Xiaodong Li, Changgui Song, Yuanqi Han, Jingyu Wang, Changyao Niu, and Xiaona Cui

School of Environment and Safety Engineering, North University of China, Taiyuan 030051, China

Correspondence should be addressed to Xiaodong Li; lixd78@126.com

Received 11 May 2022; Revised 27 July 2022; Accepted 6 August 2022; Published 28 August 2022

Academic Editor: Mazeyar Parvinzadeh Gashti

The preparation of ultra-fine energetic materials still faces great challenges. In order to prepare the ultra-fine NTO crystals with controllable size and morphology, the study proposes a novel ultrasonic-assisted spray technology that can ensure the rapidity and safety of the preparation of ultra-fine NTO crystals. The as-prepared NTO crystals are characterized by scanning electron microscopy (SEM) and X-ray diffraction (XRD), and the effects of solvent type, solution concentration, ultrasonic parameters, and anti-solvent on the morphology and average size of NTO crystals are investigated. The results obtained show that NTO ultra-fine crystals with an average particle size of 0.2 μm can be obtained quickly in optimum preparation conditions. The effectiveness of the technique presented for preparing ultra-fine spherical NTO crystals was demonstrated by comparison with baseline experiments. Ultrasonic-assisted spray technology offers a safe and fast route for the preparation of ultra-fine NTO particles and reveals an ideal method for the preparation of other ultra-fine energetic particles.

1. Introduction

3-nitro-1,2,4-triazole-5-one (NTO) is a low-sensitivity and high-density explosive whose detonation pressure and velocity are comparable to 1,3,5-trinitroperhydro-1,3,5-triazine (RDX), and its shock sensitivity and mechanical sensitivity are significantly better than RDX and octahydro-1,3,5,7-tetranitro-1,3,5,7-tetrazocine (HMX), second to triaminotrinitrobenzene (TATB) [1–4]. Due to its good performance in terms of sensitivity and energy, NTO has a great potential for application in the field of energetic materials [5–8]. However, the irregular morphology and large particle size of the raw NTO lead to its poor molding performance and low charge density, which further limits its application in mixed explosives [9, 10]. At present, nano-energetic materials have obvious advantages in improving the burning rate and explosive performance of propellants and enhancing the mechanical strength of formulations, which means greater energy density, higher stability, and safety [11–15]. Therefore, these above comprehensive factors have aroused great interest of researchers. It is reported that after recrystallization, the morphology of NTO is changed from rod to cube, the mechanical sensitivity is decreased, and the detonation velocity is increased [16, 17]. In addition, NTO crystals with regular morphology are easy to fill, and the gap between particles is small, which increases the density of charge and the energy released per unit volume, thus improving the performance of mixed explosives to a certain extent [18–21]. Consequently, preparing NTO particles that are characterized by smaller particle sizes and more regular morphology has become the focus of many researchers.

At present, ultra-fine crystals can be obtained via mechanical action such as air-jet grinding or vibrating ball milling [22, 23]. However, the water solubility of NTO and the strong vibration or friction generated by such mechanical action during the preparation process will increase the risk in the preparation process. Previously, spherical NTO particles with an average particle size of 200 μm and 500 μm [24] and cubic

NTO crystals with an average particle size of 2 μm were prepared by the cooling crystallization method and supercritical anti-solvent method, respectively [25]. However, the optimal target pressure required by the latter is 5 MPa, which poses new challenges to the performance of the devices used in the experiment to support the pressure. Subsequently, solution-anti-solvent method with mild preparation conditions is used to prepare the ultra-fine NTO crystals. Kayser et al. blew NTO/DMSO solution atomized in an inert gas into dichloromethane to prepare spherical NTO crystals with an average particle size of 0.55 mm [26]. NMP solution dissolving NTO crystals was dropped into cold water and then was quickly stirred by Hou He et al. to prepare NTO crystals with regular crystal shape and an average particle size of 40 μm [27]. However, due to intermittent operation, there was a gradual decrease in supersaturation of these two methods, which caused the formation of large crystals with uneven grain size distribution. To solve this problem, Wang Jingyu et al. proposed the micro-agglomeration dynamic crystallization method that is to make the supersaturation of solution and solvent constant in the crystallization process and then obtain products with narrow crystal size distribution [28].

At the same time, it appears that controlling the supersaturation in the crystallization process can inhibit the growth of crystals, which is beneficial to the formation of small-size crystals to a certain extent [29–33]. Therefore, based on the superfine technology mentioned above, it will be conductive that the preparation of ultra-fine NTO crystals will be possible if preparation methods can achieve a continuous high supersaturation state while enhancing the mixing degree of solvent and anti-solvent. Some studies have showed that ultrasonic wave, as an energy source, can induce nucleation at lower supersaturation and achieve a continuous supersaturation state to a certain degree [34–36]. Compared with conventional stirring, it reduces the metastable zone width and the induction time required for crystallization start and leads to rapid and uniform mixing, thus improving crystal morphology and crystal size distribution and reducing the agglomeration [37, 38]. By adjusting ultrasound-related variables such as the power density, ultrasonic duration time, and appropriate crystallization conditions, the average crystal size and its distribution can be effectively controlled. For example, Y. H. Kim et al. found that the size of NTO crystals obtained by ultrasonic radiation is changed from 140~160 μm to 30~70 μm, compared with that obtained by traditional mechanical agitation [16]. Lee et al. found that sonication during the cooling crystallization of NTO crystals had a significant effect on the crystal morphology and size distribution and lower ultrasonic frequency and ultrasonic time facilitated the generation of small-sized particles with smaller crystal size distribution [17]. Ma et al. found that ultrasound was an important factor affecting the formation of ultra-fine AP crystals, which were 0.84 μm smaller than crystals prepared without ultrasound assistance [39]. The use of ultrasonic radiation makes it possible to obtain products with the desired narrow particle size distribution and effectively eliminate the extra processing processes, which are particularly desired in industrial production. In the case of ultrasonic crystallization using ultrasonic horn, the radiation is directly propagating into the solution in the reactor through directly immersing the tip of the horn into the solution. There has been an evidence that the average particle size of crystal obtained by ultrasonic horn was smaller than that of the conventional indirect ultrasonic radiation under the level of the equivalent power dissipation, which were 146 μm and 205 μm, respectively [40].

After careful study of related articles, there is no research on the preparation of sub-micro NTO crystal by ultrasound to study its influence on the morphology and average particle size of NTO crystals. In this study, a novel injection mixing system combined with ultrasonic technology for the preparation of ultra-fine NTO crystals was proposed, and the effects of solvent type, solution concentration, ultrasonic parameters, and anti-solvent on the morphology and average particle size of ultra-fine NTO particles were studied in detail. Therefore, the current work is novelty and promising. To demonstrate the effect of the novel ultrasonic-assisted spray technique presented, the NTO crystals were recrystallized without ultrasound and using drop-wise addition as the baseline experiments, respectively. In general, this method avoids the possibility of strong vibration, strong friction, and excessively long time (1 ~ 6 h) in the process of preparing ultra-fine crystals by air-jet grinding and vibrating ball milling [41–43]; provides a safe and fast synthetic route for the preparation of NTO ultra-fine particles; and provides a new ideal method for the preparation of other high-energetic ultra-fine particles.

2. Materials and Methods

2.1. Materials. NTO was provided by Gansu Yinguang Chemical Industry Group Co., Ltd. Anhydrous ethanol was provided by Tianjin Beichen Founder Reagent Factory. Dimethyl sulfoxide, N,N-dimethylformamide, and N-methyl pyrrolidone were purchased from Tianjin Fengchuan Chemical Reagent Technology Co., Ltd. Dichloromethane and 1,2-dichloroethane were provided by Sinopharm Group Chemical Reagent Co., Ltd. All of these analysis-grade reagents were used without further purification. JY92-IIDN ultrasonic cell crusher and CK-4007GD rapid high and low temperature-programmed thermostatic tank were purchased from Xinzhi Biotechnology Co., Ltd. (Ningbo, China); FD-1A-50 freeze-drying machine was provided by Beijing Boyikang Technology Company, China.

2.2. Instruments. Figure 1 shows the schematic of the experimental apparatus for NTO solvent-anti-solvent crystallization using a novel injection mixing system combined with ultrasonic technology. In order to facilitate operation and control variables, the liquid height is always restricted to 2/5 of the reactor that consists of a flat bottom jacketed reactor with a capacity of 250 mL. The self-made nozzle, which connected to the external air pump, is fixed above the reactor through a metal bracket, and the NTO solution in the nozzle can be completely sprayed into the reactor under the pressure of the air pump by adjusting the angle between the nozzle and reactor. The frequency of the ultrasonic crusher is 20 KHz, the power can be adjustable from 5 to 500 W, and the ultrasonic horn is immersed into 1/3 of the lowest liquid level. As shown in Figure 1, the magnetic stir installed at the bottom inside the reactor stirs the solution at a certain

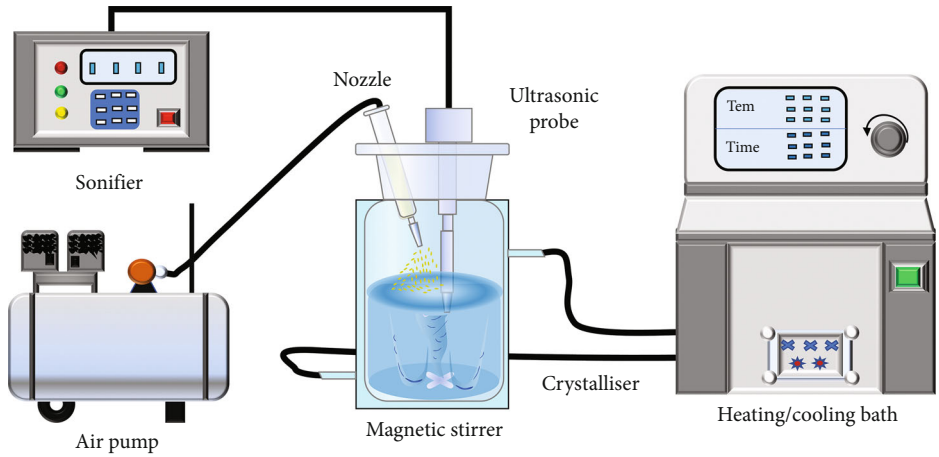

Figure 1: A schematic of the apparatus used in the experiments.

speed so as to further increase the mixing degree and speed. And the device is connected with a constant temperature tank to control the temperature of the crystallization process.

2.3. Synthesis and Experimental Procedure. DCM (quantity depends on solvent and anti-solvent ratio) was taken in the jacketed reactor, and the bath temperature was maintained as desired. The anti-solvent, that is, the organic reagent that cannot dissolve NTO, but is intersoluble with the solvent that can dissolve NTO, is stirred at a medium speed with a magnetic stirrer for a period of time to ensure that its temperature reaches the preset bath temperature, and the ultrasonic horn is immersed in 1/3 of the liquid. And then, the NTO crystals (the amount depends on the concentration) were added into the 6 mL DMF, stirred in a water bath at 70 °C until completely dissolved, and poured into a spray bucket with a nozzle diameter of 0.5 cm. Turn on the air pump, adjust the output pressure of the air pump to 0.5 MPa, align the nozzle to the midpoint between the horn and the wall of the reactor, and spray the DMF solution with NTO into the rapidly stirring liquid. Ultrasound was applied as soon as the addition of solution to anti-solvent and the ultrasonic intensity was set to 30 W. Finally, the suspension containing NTO crystals was obtained, filtered and washed several times, and then freeze-dried for 6 h.

Figure 2 shows the schematic diagram of the ultra-fine NTO crystal obtained when the NTO solution is sprayed into the anti-solvent under the action of ultrasound. The formation of ultra-fine spherical NTO crystals with smooth surface and regular morphology can be explained from the following two aspects. On the one hand, sonocrystallization relies on instantaneous cavitation, which leads to the formation of transient cavities (bubbles) and eventually leads to catastrophic collapse. This occurs when the cavity is filled with vapor rather than gas and results in the release of a large amount of localized energy, which then goes through a phase of rapid temperature decline, eventually leading to the generation of a significant number of crystal nuclei [44]. With the increase of nucleation, more crystal nuclei appear in the form of increasing crystal surface area, which leads to an increase in solute consumption caused by growth phenomena. Supersaturation and continuous crystal growth are distributed in the formed nuclei, resulting in large numbers of smaller particles [45]. On the other hand, with the increase of nucleation, the collision probability between NTO crystals and between crystals and the device wall increases so that the agglomeration between the fine crystals is destroyed, the large-grain crystals are difficult to maintain, and the crystals with rough surface or irregular morphology are polished, resulting in reduced particles size and gradually regular or spherical morphology of NTO particles [46, 47].

According to the above experimental steps, the experiment without ultrasonic addition is baseline experiment 1, and the experiment in which NTO crystals were recrystallized by drop-wise addition method without the spraying technique is baseline experiment 2.

2.4. Sample Characterization. The morphology of NTO crystals was characterized by scanning electron microscopy (SEM, Tescan Mira3 LMH, Czech). The size distribution of NTO crystals was analyzed by ImageJ software. Again, repetitive analysis has been done to obtain repeatable results of particle size distribution and average particle size reported in the work. X-ray diffraction (XRD, Dandong Haoyuan DX-2700, China) was used to investigate the crystal form of raw NTO and recrystallized NTO.

3. Results and Discussion

In order to demonstrate the effectiveness of the novel ultrasonic-assisted spray technology, the effects of solvent type, solution concentration, ultrasonic parameters, and anti-solvent on the morphology and average particle size of ultra-fine NTO particles were studied in detail. Meanwhile, NTO crystals were recrystallized without ultrasound and by drop-wise addition, respectively.

3.1. Effect of Solvents on NTO Crystals. On the basis of the selection principle of solvent and anti-solvent, the physical and chemical properties such as solubility, viscosity, and boiling point that could affect the supersaturation transport process, diffusion, and crystal growth should be studied in the case of anti-solvent recrystallization. Additionally, different solvents may be preferred to adsorb on different crystal

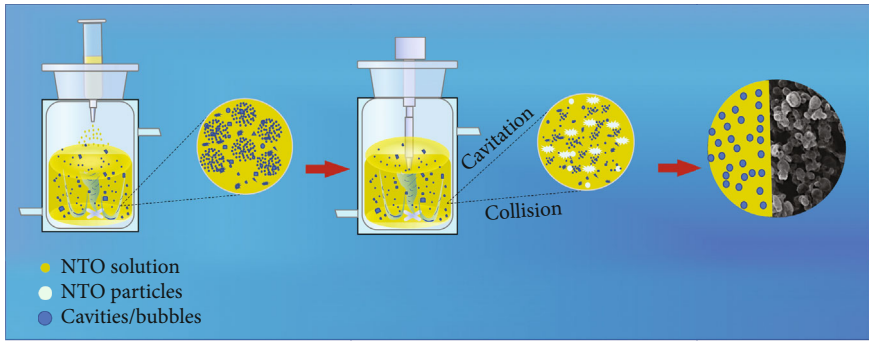

Figure 2: Schematic illustration of the formation of ultra-fine NTO crystal.

surfaces, which directly lead to some differences in crystal size, morphology, and other aspects. Therefore, it is very important to select a suitable solvent-anti-solvent system for obtaining the ideal morphology of NTO crystals.

3.1.1. Effect of Different Solvents on NTO Crystals. Table 1 and Figure 3 show the average size and SEM images of NTO particles obtained by recrystallization with different solvents, respectively. Among them, when DMF was used as the solvent, polyhedral morphology was also observed, and the average particle size of the crystal was 0.20 μm. Thus, DMF, which resulted in the smallest average particle size and the most regular morphology, was used as the solvent in this study. The XRD test was conducted on samples to determine whether the crystal phase transformation of NTO occurred during recrystallization in different solvents. Figure 4 is the XRD patterns of the raw NTO and NTO crystals recrystallized in different solvents. The results show that the crystal form has not been changed according to the analysis of the Jade9.0 and pdf-2009 databases (PDF 54-1529). It can be seen from Figure 4 that the diffraction peak intensity of the recrystallized NTO crystal is significantly lower than that of the raw material, because with the decrease of particle size, the X-ray diffraction peak intensity gradually weakens or even disappears [47, 48]. Meanwhile, there are significant differences in the diffraction peak intensity and peak width of recrystallized NTO crystals in different solvents at the same diffraction angle, indicating that the type of solvent affects the crystal morphology and particle size of NTO crystals, which is consistent with that observed in Figure 3. Among them, most of the diffraction peak intensities of the NTO crystals obtained by using DMF as a solvent are lower than those obtained by recrystallization from other solvents, indicating that the particle size of the crystals obtained by using DMF as a solvent is significantly smaller.

3.1.2. Effect of Solution Concentration on NTO Crystals. When the temperature is constant, the solution concentration directly determines the degree of supersaturation. As the driving force of the crystallization process, it mainly affects the speed of nucleation formation and crystal growth and then indirectly controls the size and morphology of crystal. The control experimental conditions were as follows: DMF-DCM as crystallization system, the ultrasonic intensity of 5%, ultrasonic time of 15 min, crystallization temperature of 5 °C, and

Table 1: Morphology and crystal size of NTO crystals obtained using different solvents.

Solvent	Morphology	Average particle size (μm)
DMSO	Cuboid	1.25
NMP	Irregular	0.43
DMF	Polyhedral	0.20
V_{DMSO}[a]:V_{DMF}[a] (2 : 1)[b]	Cuboid	4.47
V_{DMSO}:V_{DMF} (1 : 1)[b]	Cuboid	1.62
V_{DMSO}:V_{DMF} (1 : 2)[b]	Irregular	1.28

[a] V_{DMSO} and V_{DMF} refer to the volume of DMSO and DMF; [b]V_{DMSO}:V_{DMF} (2 : 1), V_{DMSO}:V_{DMF} (1 : 1), and V_{DMSO}:V_{DMF} (1 : 2) refer to the volume ratio of DMSO to DMF that is 2 : 1, 1 : 1, and 1 : 2, respectively.

solution concentration of 0.2, 0.4 g•mL^{-1} and 0.6 g•mL^{-1}, respectively.

The refined NTO was characterized by scanning electron microscopy (SEM), and the results were shown in Figure 5. It can be seen from the Figure 5 that when the solution concentration increased from 0.2 g•mL^{-1} to 0.4 g•mL^{-1}, the median particle size of NTO crystals changed from 0.65 μm rod-like crystals with a length-diameter ratio of 1:3 to 0.2 μm spherical particle with a uniform particle size distribution. These results can be proved by the dependence of nucleation process on solution concentration and temperature. When the crystallization temperature is constant, higher concentrations of solution is more inclined to produce higher supersaturation degree upon the mixing with the anti-solvent, which affects the growth rate of crystal and accelerates the formation of crystal nucleus. When the solution concentration is 0.6 g•mL^{-1}, higher solution concentration slows down the diffusion speed of particles to the nucleus and the contact speed with the surface of the nucleus, leading to the direct dissolution of some NTO particles back into the solvent system, thus making the nucleus grow up and causing serious particle agglomeration. At the same time, the viscosity of the solution will increase with the increase of concentration, which is not conducive to uniform mixing with anti-solvents, resulting in irregular morphology and uneven particle size of the final product. Therefore, the solution concentration was set to 0.4 g•mL^{-1}.

3.2. Effect of Ultrasound on NTO Crystals. Almost all theories agree that the effect of ultrasonic waves in the crystallization

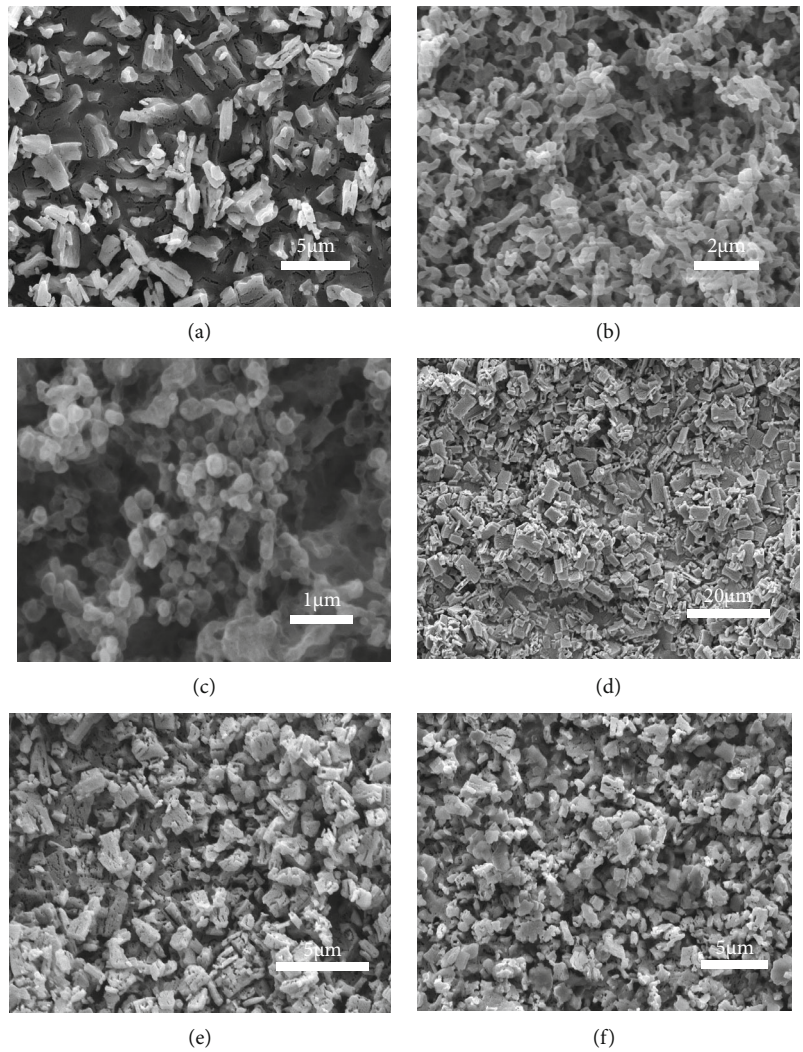

Figure 3: SEM images of NTO crystals prepared with different solvents. (a) DMSO; (b) NMP; (c) DMF; (d) V_{DMSO}:V_{DMF} (2 : 1); (e) V_{DMSO}:V_{DMF} (1 : 1); (f) V_{DMSO}:V_{DMF} (1 : 2).

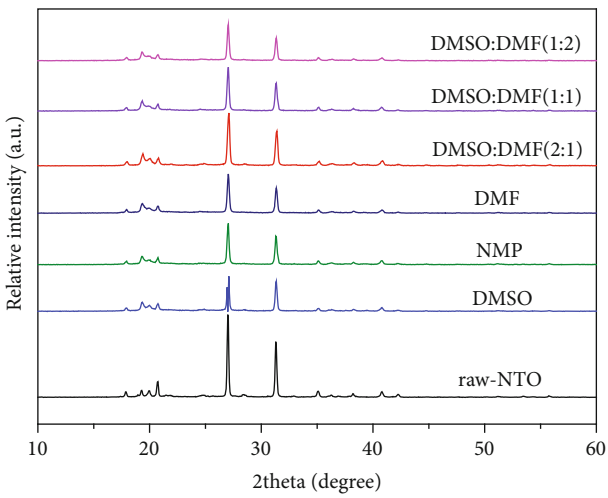

Figure 4: XRD spectra of NTO crystals prepared in different solvents.

process is caused by cavitation, which is the most important activity in the process of acoustic crystallization due to the pressure fluctuations generated by ultrasonic waves causing voids in the liquid. It contributes to achieve reproducible particle nucleation at lower supersaturation levels and form a more uniform particle size and morphology. Firstly, sonocrystallization depends on transient cavitation, forming a short-lived cavity (bubbles) that eventually leads to catastrophic collapse and a large amount of local energy release. Secondly, it goes through a phase of sharp temperature drops, which eventually leads to the production of a large number of nuclei. In this work, the crystallization process was explored by changing the parameters affecting cavitation like ultrasonic power, ultrasonic duration, and temperature. According to the experimental results, the effects of different operating parameters on the sonocrystallization of NTO were discussed.

3.2.1. Effect of Ultrasonic Power on NTO Crystals. In the safe range of experimental operation, the effect of ultrasonic power was investigated using five different ultrasonic power levels of 0, 12, 30, 60, and 90 W, respectively, where the ultrasonic

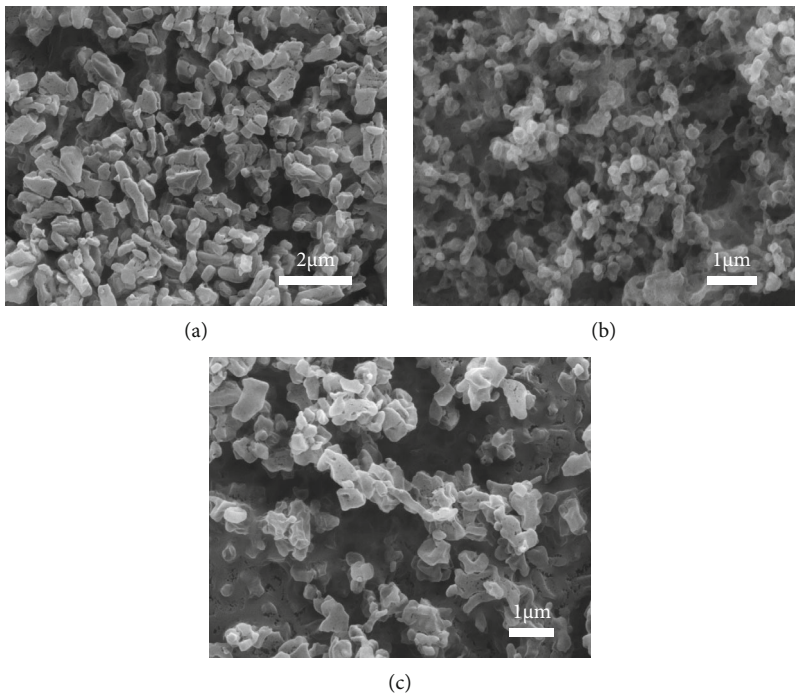

Figure 5: SEM images of NTO crystals prepared with different DMF concentrations. (a) 0.2 g•mL^{-1}; (b) 0.4 g•mL^{-1}; and (c) 0.6 g•mL^{-1}.

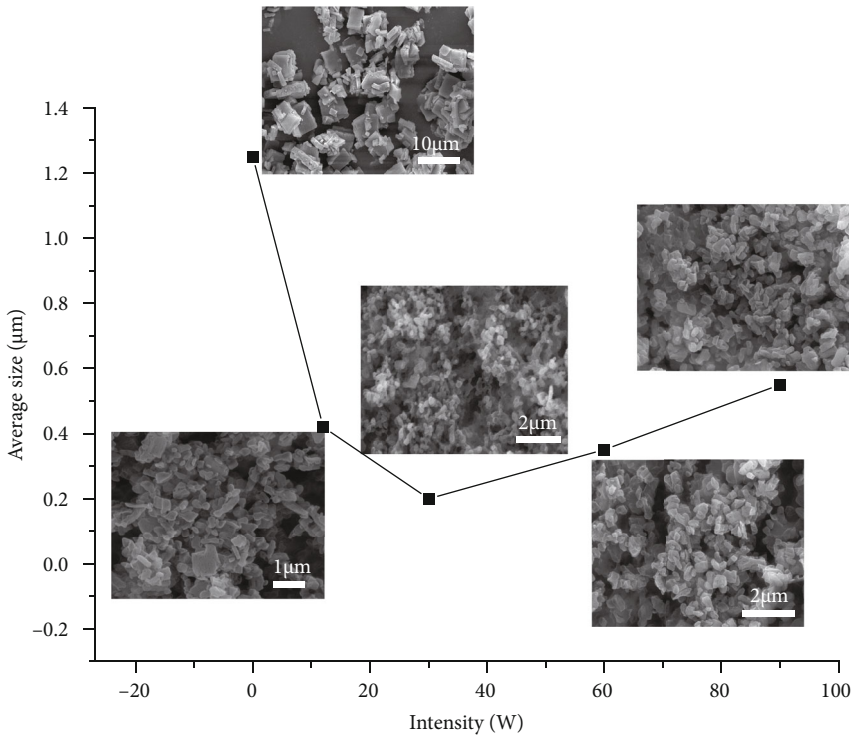

Figure 6: Variation of average particle size of NTO crystals with ultrasonic power.

power is 0 as the baseline experiment 1. Figure 6 shows that when the ultrasonic power is 0, that is, there is no ultrasonic effect, the average particle size of plate NTO crystals with 1.25 μm were obtained by the spraying technology, which is 0.7 μm larger than the average particle size of the largest particle size obtained under the ultrasonic action, indicating that the introduction of the ultrasonic system greatly reduces the particle size, and that ultrasonic is an important factor affecting the formation of ultra-fine NTO crystals. Before attaining 30 W, there was a significant decrease in the average particle

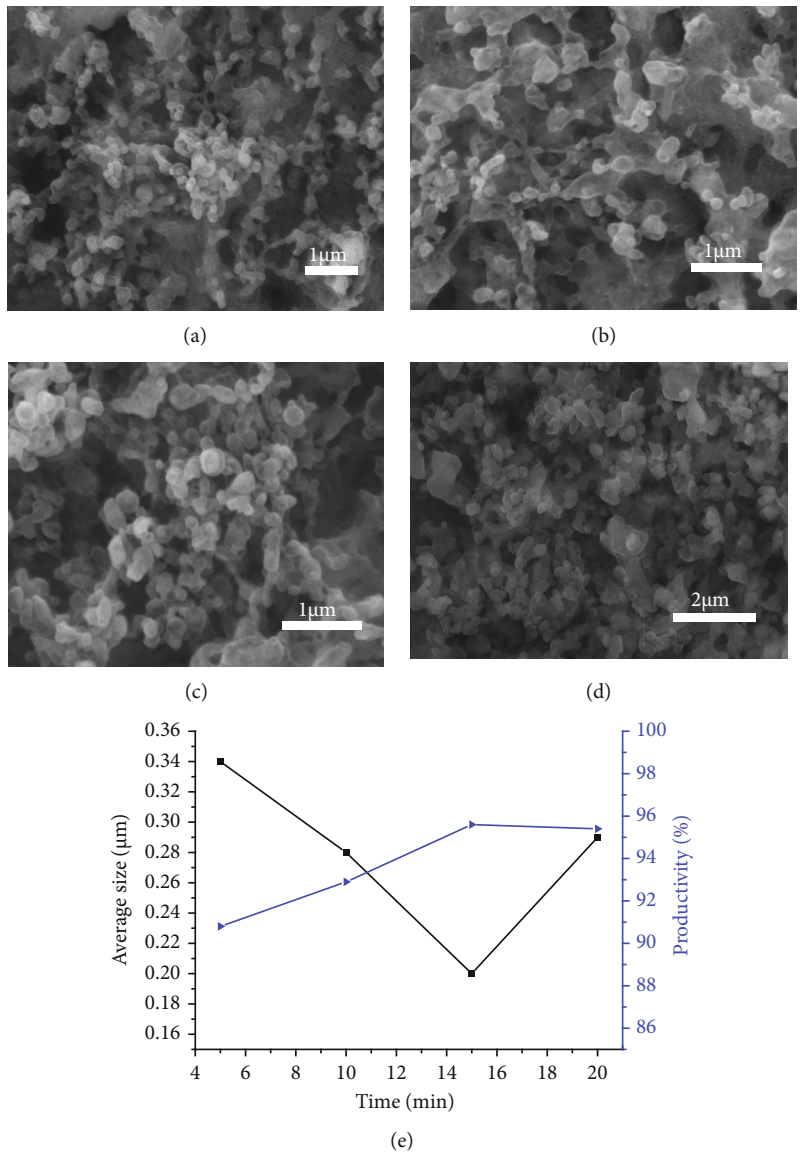

Figure 7: SEM images of NTO crystals prepared in various ultrasonic times. (a) 5 min; (b) 10 min; (c) 15 min; (d) 20 min; and (e) average particle size and productivity of NTO crystals and as a function of ultrasonic time.

size with increasing ultrasonic power. This result can be attributed to the fact that with the increase of ultrasonic power, the hole effect and the system supersaturation gradually are strengthened, which further shorten the induction time and the metastable zone, thus strengthening the mass transfer and diffusion between the systems and finally promoting the formation of small-sized crystals. Meanwhile, the periodic oscillation waves generated by ultrasonic are dispersed more evenly in the system, which means that the crystal nucleus will grow more evenly. After 30 W, with the increase of ultrasonic power, the crystal morphology became more irregular and agglomerated, and the average particle size of the crystal also increased to 0.35 μm and 0.55 μm, respectively. Excessive ultrasonic power will cause the strength movement of molecules, which is not conducive to the formation of crystal nucleus. At the same time, ultrasonic dispersion makes particles rotate at high speed in the form of energy and collide with the wall of the reaction kettle, and due to the different crystal faces subjected to different sizes of forces, the growth rate of each crystal face become different, resulting in irregular crystal morphology. When the ultrasonic power was set above 90 W, it was found that the liquid splashed on the reactor wall, causing some problems and unforeseen dangers in the whole crystallization operation. Therefore, the power of ultrasonic waves in crystallization process should not be set too high.

3.2.2. Effect of Time of Application of Ultrasound on NTO Crystals. The experiment of ultrasonic time variation was carried out under the conditions of solution concentration of 0.4 g•mL^{-1}, operating temperature of 5 °C, ratio of solution to anti-solvent of 1 : 15, and ultrasonic power of 30 W. Figure 7 shows the effect of ultrasound on crystal morphology and yield. It was found that with the increase of ultrasonic irradiation time, the particle size changed, and the yield of precipitated

crystals increased gradually. As shown in Figure 7, when the ultrasonic irradiation time was 15 min, the average particle size of NTO crystals was the smallest, which first significantly decreased and then slightly increased with the increase of ultrasonic irradiation time. This is because when the ultrasonic irradiation time is short, the effect of cavitation on nucleation rate and the width of metastable interval is weak, leading to a lower yield of precipitated crystals, which leads to a larger distance between the corresponding crystal nuclei and a lower probability of particle collision, thus obtaining crystals with larger grain size. With the increase of irradiation time, the number of crystals precipitated increases, which increases the probability of collision between crystals, between crystals and the wall and between crystals and the ultrasonic horn. The experimental results show that the particle size decreases, and the morphology becomes regular and spherical gradually. However, when the ultrasonic radiation lasted for a long time, the crystal was constantly under high supersaturation, and the number of particles per unit volume increased. The particles were rapidly aggregated without dispersing. Therefore, they grew to a larger extent and formed crystals with larger grain size, as shown in Figure 7(d). By controlling the operation time, the grain size can be effectively controlled, and the yield can be controlled within a reasonable range under the premise of getting a smaller grain size.

3.2.3. Effect of Ultrasonic Temperature on NTO Crystals. Considering that the boiling point of anti-solvent dichloromethane is 312.75 K, an external programmable thermostatic tank was used to set the temperature at 253.15, 268.15, 273.15, 278.15, 283.15, and 288.15 K, respectively, within the safe range of experimental operation to study the influence of ultrasonic temperature on the average particle size and morphology of NTO crystals. Figure 8 shows that with the increase of ultrasonic temperature, the average particle size of NTO crystals becomes more irregular. Figure 8(a) is the fitting curve of the size distribution of NTO crystals. The results show that when the ultrasonic temperature is higher than 278.15 K, the particle size gradually decreases, and the particle size distribution becomes narrower of the NTO crystal with the decrease of the temperature. When the ultrasonic temperature is lower than 278.15 K, with the increase of the temperature, the particle size and particle size distribution of NTO crystals show the same trend as above. To determine the optimal conditions, the average particle size data (Figure 8(b)) at each temperature were drawn towards the determination of the optimal conditions, and the minimum particle size was again achieved, this time at a temperature of 278.15 K. The trend in Figure 8(b) shows that lower temperatures do contribute to the reduction of the average crystal size. This is due to the fact that lower temperature can inhibit the growth of crystals, which is conducive to the production of small diameter crystals. The higher temperature will make the crystallization rate of the crystal unstable, resulting in a large difference in the size of the particle size, but also cause the irregular crystal morphology. Lowering the temperature is expected to have an opposite effect on particle size and explained as follows: Lowering the temperature will increase the viscosity of the liquid, and the increase in viscosity will increase the natural cohesion force acting on the liquid, thus increasing the magnitude of the cavitation threshold, which means that cavitation is more difficult to form and is not conducive to nucleation under cavitation. Moreover, when the crystallization temperature is low, the supersaturation of the solution is relatively high, which leads it easy to precipitate nuclei but insufficient growth of crystals. Therefore, crystals with small particle sizes but irregular morphology are easy to be obtained, and the refining effect is not obvious. Thus, the selection of an appropriate low-temperature range is helpful to disperse the heat generated in the recrystallization process and is of great significance for the preparation of small grain size with regular morphology. Having said all of above, the ultrasonic temperature was set to 278.15 K.

3.3. Effect of Anti-Solvent on NTO Crystals. The principle of anti-solvent recrystallization is actually the process of the solvent and the anti-solvent seizing the solute. It takes advantage of the insolubility of solute in anti-solvent to achieve higher supersaturation and make the solute crystallizes. Thus, the effect of anti-solvent on the particle size of NTO crystals can be expressed by the type of anti-solvent and the volume ratio of anti-solvent to that of the solution.

3.3.1. Effect of the Volume Ratio of anti-Solvent to Solvent on NTO Crystals. The volume ratio of anti-solvent to that of the solution directly affects the supersaturation of recrystallization in the system and then determines the metastable zone in which the solution is located. Different metastable regions will determine the nucleation and growth of crystals how and then affect the morphology and particle size distribution of the obtained crystal particles and also have a certain influence on the uniformity of the crystal. Figure 9 shows that with the increase of the volume ratio of non-solvent to solvent, the average particle size of NTO crystal first decreases and then remains unchanged, and the most prominent is that the volume ratio of non-solvent to solvent is 15 : 1, which is regarded as nodule. This is due to the fact that the volume of the anti-solvent is one of the factors that determine the supersaturation of the solution. The smaller volume ratio will reduce the distance between the crystal nuclei and the collision probability between explosive particles, in order that the explosive particles without collision agglutinate directly towards the crystalline nuclei, giving an irregular crystalline morphology and a larger crystalline size. As the ratio of anti-solvent to solvent increases, the probability of collision between explosive particles increases, and the speed of agglomeration toward the crystal nucleus accelerates, which makes the irregular crystal broken, and then crystals with relatively ideal morphology are obtained. When the ratio increases to a certain extent, the velocity of particle diffusion towards the crystal nucleus and contact with the surface of the crystal nucleus gradually decreases, and some explosive particles are dissolved back into the solution again. In this repeated process, the crystal nucleus continues to grow, and then the grain agglomeration occurs, which makes the product morphology irregular. At that time, the level of

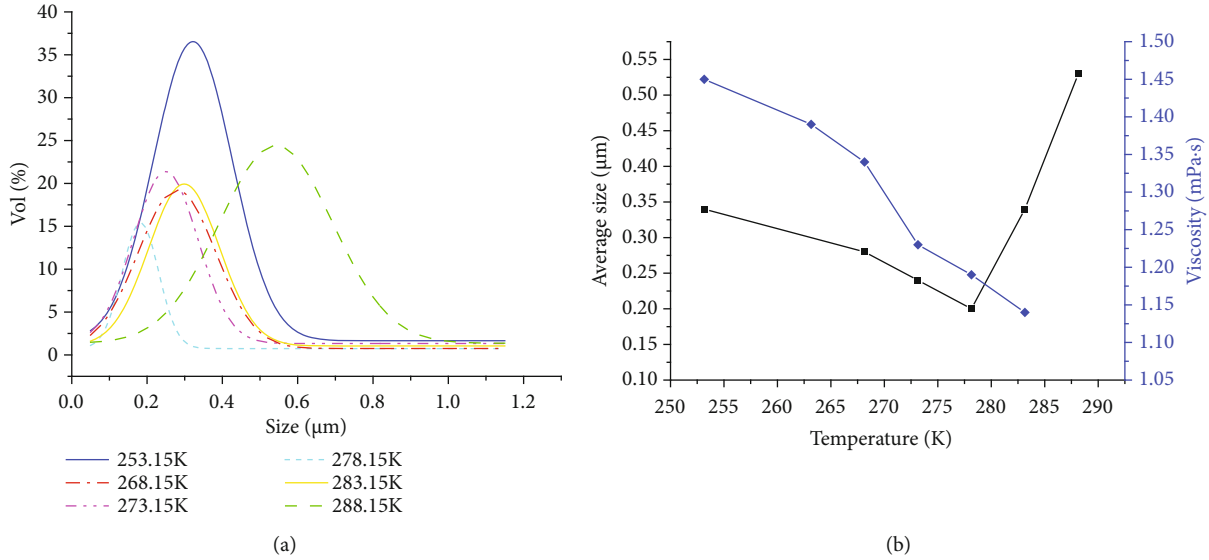

Figure 8: Variation of NTO crystal particle size with ultrasonic temperature. (a) NTO crystal size distributions. (b) Average particle size of NTO crystals and the viscosity of DMF and as a function of ultrasonic temperature.

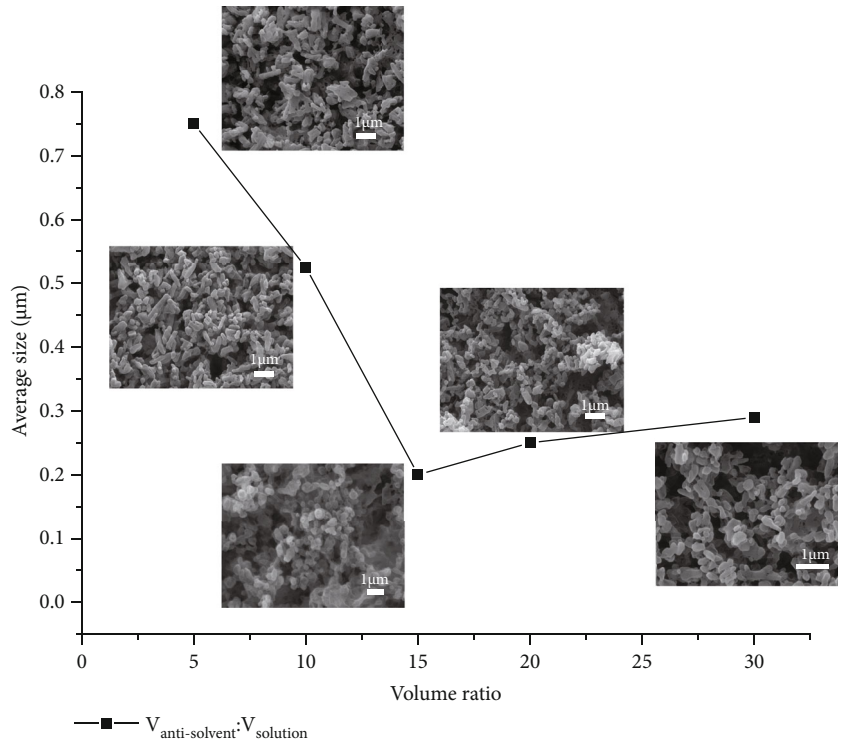

Figure 9: Variation of the average particle size of NTO crystals varies with the volume ratio of anti-solvent to solvent.

nucleation and crystallization tended to be limited; therefore, no further decreases were observed.

3.3.2. Effect of Different Anti-Solvents on NTO Crystals. Through the above experiments, combined with the selection principle of anti-solvent, DMF was used as solvent to explore the influence of DCM, 1,2-dichloroethane (EDC) and distilled water as anti-solvents on the crystal morphology and particle size of NTO, and the results are shown in Figure 10. By adjusting various experimental parameters, spherical NTO crystals with an average particle size of 0.2 μm were obtained using DCM as a non-solvent. Irregular NTO crystals with large particle size distribution and average particle size of 0.4 μm were obtained by using EDC as

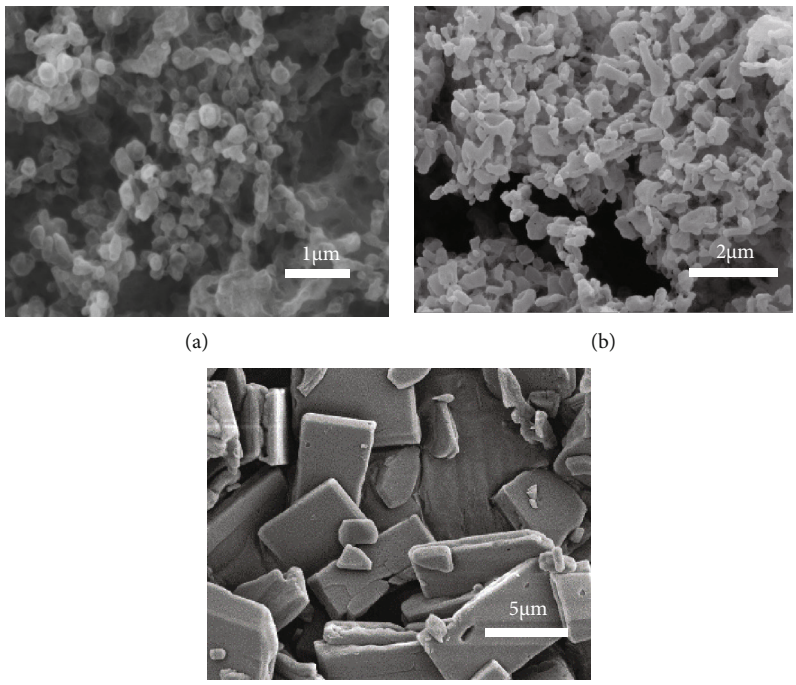

Figure 10: SEM images of NTO crystals prepared with different anti-solvents. (a) DCM; (b) EDC; and (c) distilled water.

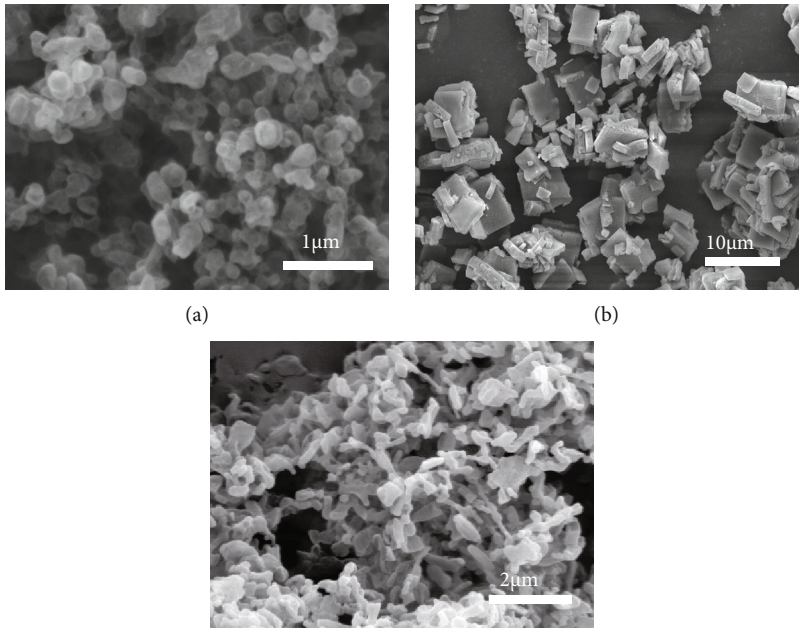

Figure 11: SEM images of NTO crystals prepared in the novel ultrasonic-assisted spray technique (a), the baseline experiment 1 (b), and the baseline experiment 2 (c).

a non-solvent, as shown in Figure 10(b). When the ultrasonic temperature is adjusted to 275.15 K, the solubility of NTO in water is less than 1 g/100 g, which is slightly soluble, which is in line with the principle of anti-solvent selection. At this time, smooth surface sheet-like NTO crystals with an average particle size of 8 μm were obtained, as shown in Figure 10(c). Thus, DCM, which resulted in the smallest average particle size and the most regular morphology, was used as the anti-solvent in this study.

To further demonstrate the effect of the technique presented, NTO particles were recrystallized in baseline experiment 1 (without sonication) and baseline experiment 2 (by

the drop-wise method) respectively. Figure 11(a) shows the spherical NTO particle with an average particle size of 0.2 μm obtained under the optimal experimental parameters using the novel ultrasonic-assisted spray technology. When the ultrasonic power is 0, that is, there is no ultrasonic effect; the average particle size of plate NTO crystals with 1.25 μm was obtained by the spraying technology, which is 0.7 μm larger than the average particle size of the largest particle size obtained under the ultrasonic action, as shown in Figures 6 and 11(b). When the NTO was recrystallized by the drop-wise method rather than by the spray system, NTO crystals with an average particle size of 0.43 μm and irregular morphology were obtained, which were 0.23 μm larger than the minimum particles obtained by the novel ultrasonic-assisted spray technology, as shown in Figures 11(a) and 11(c). The results show that the introduction of the ultrasonic system and the spray system both reduced the particle size to a certain extent, but the NTO crystal was still larger than that obtained by the novel ultrasonic-assisted spraying technology, and the morphology was irregular, illustrating the effectiveness of the technique presented to prepare ultrafine spherical NTO crystals.

4. Conclusion

The present experiments show that submicron spherical NTO particles with an average particle size of 0.2 μm were obtained by a novel ultrasonic-assisted spray technique using a solvent-anti-solvent method. The morphology and particle size of NTO crystals were found to be closely related to the experimental parameters such as solvent type, solubility, ultrasonic parameters, and anti-solvent. By adjusting the experimental parameters, spherical NTO crystals with an average particle size of 0.2 μm were obtained under the optimal process parameters, that is, when the solvent is DMF, the nonsolvent is DCM, the solution concentration is 0.4 g•mL^{-1}, the ultrasonic power is 30 W, the ultrasonic time is 15 min, the ultrasonic temperature is 278.15 K, and the volume ratio of anti-solvent and solvent is 15. In addition, compared with the baseline experiments, it was found that the introduction of the ultrasonic system and the spray system reduced the particle size to a certain extent, but it was still larger than the NTO crystals obtained by the new ultrasonic-assisted spray system, and the morphology was irregular, which indicated the effectiveness of the technology presented to prepare ultra-fine spherical NTO crystals. In general, the ultrasonic-assisted spray technology provides a safe and fast synthetic route for the preparation of ultrafine NTO particles and provides an ideal method for the preparation of other ultra-fine energetic particles.

Data Availability

The data used to support the findings of this study are available from the corresponding author upon request.

Conflicts of Interest

The authors declare that there is no conflict of interest regarding the publication of this paper.

References

[1] K. Y. Lee, L. B. Chapman, and M. D. Cobura, "3-nitro-1,2,4-triazol-5-one, a less sensitive explosive," *Journal of Energetic Materials*, vol. 5, no. 1, pp. 27–33, 1987.

[2] G. Tang, X. Wang, and Z. Liu, "Research on cast PBX explosive containing NTO," *Chinese Journal of Explosives & Propellants*, vol. 1, pp. 14–18, 1995.

[3] C. Hua, M. Huang, H. Huang, J. S. Li, F. D. Nie, and B. Dai, "Intragranular defects and shock sensitivity of RDX/HMX," *Chinese Journal of Energetic Materials*, vol. 18, no. 2, pp. 152–157, 2010.

[4] Y. Li, J. Li, J. Zhang, L. Pan, and R. Xu, "Shock sensitivity of HMX-based pressed PBX at high relative density," *Chinese Journal of Explosives & Propellants*, vol. 34, no. 5, pp. 43–45, 2011.

[5] H. Guo, X. Yu, T. Ding, Y. Zhao, and X. Yang, "Effect of the NTO content on the mechanical sensitivities and detonation velocity of RDX based aluminized explosives," *Chinese Journal of Explosives & Propellants*, vol. 38, no. 5, 2015.

[6] Z. Y. Can, A. Uzer, Y. Tekdemir, E. Erçağ, L. Türker, and R. Apak, "Spectrophotometric and chromatographic determination of insensitive energetic materials: HNS and NTO, in the presence of sensitive nitro-explosives," *Talanta*, vol. 90, pp. 69–76, 2012.

[7] X. Li, B. Wang, and Q. Lin, "Compatibility study of 2,6-diamino-3,5-dinitropyridine-1-oxide with some energetic materials," *Central European Journal of Energetic Materials*, vol. 13, no. 4, pp. 978–988, 2016.

[8] Y. Liu, R. Gou, S. Zhang, Y. H. Chen, H. J. Cheng, and M. H. Chen, "Solvent effect on the formation of NTO/TZTN cocrystal explosives," *Computational Materials Science*, vol. 163, pp. 308–314, 2019.

[9] W. Yu, F. Nie, H. Huang, P. Wang, W. Li, and K. Cheng, "Morphology and structure of NTO spheroidal crystals," *Chemical Research and Application*, vol. 18, no. 3, pp. 324–326, 2006.

[10] R. Vijayalakshmi, S. Radhakrishnan, P. Shitole et al., "Spherical 3-nitro-1,2,4-triazol-5-one (NTO) based melt-cast compositions: heralding a new era of shock insensitive energetic materials," *RSC Advances*, vol. 5, no. 123, pp. 101647–101655, 2015.

[11] X. Tan, X. Duan, C. Pei, and H. L. Xu, "Preparation of nano-TATB by semibatch reaction crystallization," *Nano Brief Reports and Reviews*, vol. 8, no. 5, pp. 76–83, 2013.

[12] C. Li, S. Liu, Z. Xie, B. Ye, C. An, and J. Wang, "Design and fabrication of CL-20-based composites with an ordered close-packing structure by inkjet printing," *Colloids and Surfaces A: Physicochemical and Engineering Aspects*, vol. 639, no. 5, p. 128331, 2022.

[13] W. Wang, H. Li, Y. Yang, F. Zhao, H. Li, and K. Xu, "Enhanced thermal decomposition, laser ignition and combustion properties of NC/Al/RDX composite fibers fabricated by electrospinning," *Cellulose*, vol. 28, no. 10, pp. 6089–6105, 2021.

[14] P. Deng, Q. Jiao, and H. Ren, "Laminated ammonium perchlorate-based composite prepared by ice-template freezing-induced assembly," *Journal of Materials Science*, vol. 56, no. 3, pp. 2077–2087, 2020.

[15] H. Zhang, Y. Liu, S. Li et al., "Three-dimensional hierarchical 2,2,4,4,6,6-hexanitrostilbene crystalline clusters prepared by controllable supramolecular assembly and deaggregation process," *CrystEngComm*, vol. 18, no. 41, pp. 7940–7944, 2016.

[16] Y. H. Kim, K. Lee, K. K. Koo, Y. G. Shul, and S. Haam, "Comparison study of mixing effect on batch cooling crystallization of 3-nitro-1,2,4-triazol-5-one (NTO) using mechanical stirrer and ultrasound irradiation," *Crystal Research & Technology*, vol. 37, no. 9, pp. 928–944, 2002.

[17] H. Lee, K. Koo, S. Haam, S. H. Kim, H. S. Kim, and B. S. Park, "Effect of ultrasound on recrystallization of 3-nitro-1,2,4-triazole-5-one," *Journal of Chemical Engineering of Japan*, vol. 33, no. 6, pp. 842–847, 2000.

[18] L. Du, S. Jin, Q. Shu et al., "The investigation of NTO/HMX-based plastic-bonded explosives and its safety performance," *Defence Technology*, vol. 18, no. 1, pp. 72–80, 2022.

[19] S. K. Jangid, S. Radhakrishnan, V. J. Solani et al., "Evaluation studies on partial replacement of RDX by spherical NTO in HTPB-based insensitive sheet explosive formulation," *Journal of Energetic Materials*, vol. 37, no. 3, pp. 320–330, 2019.

[20] A. K. Hussein, A. Elbeih, and S. Zeman, "Thermal decomposition kinetics and explosive properties of a mixture based on *cis* -1,3,4,6-tetranitrooctahydroimidazo-[4,5-d]imidazole and 3-nitro-1,2,4-triazol-5-one (BCHMX/NTO)," *Thermochimica Acta*, vol. 655, pp. 292–301, 2017.

[21] G. Lan, S. Jin, M. Chen et al., "Preparation and performances characterization of HNIW/NTO-based high-energetic low vulnerable polymer-bonded explosive," *Journal of Thermal Analysis and Calorimetry*, vol. 136, no. 6, pp. 3589–3602, 2020.

[22] L. Shen, G. Li, Y. Luo, K. Gao, C. P. Chai, and Z. Ge, "Preparation of Al/B/Fe2O3 nano-composite energetic materials by high energy ball milling," *Journal of Solid Rocket Technology*, vol. 37, no. 2, pp. 233–237, 2014.

[23] H. Li, X. Cao, B. Wang et al., "Synthesis, characterization and hydroscopicity testing of molecular perovskite energetic materials," *Chinese Journal of Energetic Materials*, vol. 28, no. 6, pp. 539–543, 2020.

[24] X. Ma, Q. Hai, S. Chen et al., "A method for controlling the morphology and grainsize of NTO crystals," 2018, CN108409676A.

[25] Q. Pan and T. Chai, "Preparation study on the particle gradation of NTO with supercritical anti-solvent," *Initiators and Pyrotechnics*, vol. 2, pp. 5–8, 2007.

[26] E. G. Kayser, "Recrystallization of 3-nitro-1,2,4-triazol-5-one from dimethylsulfoxide and methylene chloride," 1991, US, USH990 H.

[27] H. Hou, W. Wu, W. Wang, H. Jia, and M. Zhang, "A preparation method of fine particle NTO," 2018, CN108997238A.

[28] J. Wang, J. Zhang, and W. Xu, "Synthesis, characterization and hydroscopicity testing of molecular perovskite energetic materials," *Chinese Acta Armamentar*, vol. 28, no. 6, pp. 539–543, 2020.

[29] H. Wang, J. Chen, L. Yao, Z. Liu, and S. Liu, "Synthesis nucleation rate of ultrafine HMX recrystallized by carbon dioxide gas anti-solvent method," *Chinese Journal of Energetic Materials*, vol. 18, no. 5, pp. 532–537, 2010.

[30] X. Wang, J. Zhang, and J. Zhang, "Ultrafine HMX prepared by solvent-nonsolvent method," *Blasting*, vol. 30, no. 3, pp. 125–128, 2013.

[31] X. Zhou, Y. Ren, H. Li et al., "Polymer-directed crystallization of HMX to construct nano-/microstructured aggregates with tunable polymorph and microstructure," *CrystEngComm*, vol. 24, no. 4, pp. 755–764, 2022.

[32] H. Lin, Z. Lei, Z. Jiang et al., "Supersaturation-dependent surface structure evolution: from ionic, molecular to metallic micro/nanocrystals," *Journal of the American Chemical Society*, vol. 135, no. 25, pp. 9311–9314, 2013.

[33] Y. Zeng, J. Cao, Z. Wang, J. Guo, and J. Lu, "Formation of amorphous calcium carbonate and its transformation mechanism to crystalline CaCO3in laminar microfluidics," *Crystal Growth & Design*, vol. 18, no. 3, pp. 1710–1721, 2018.

[34] M. Ma, B. Zhang, W. Lu, Y. Wang, X. Cao, and Y. Guo, "Investigation of ultrasonication and/or mechanical stirring on the reactive crystallization of calcium carbonate at lower temperature and higher supersaturation condition," *Journal of Crystal Growth*, vol. 570, p. 126243, 2021.

[35] C. Yang, C. Wu, and L. Shi, "Effect of ultrasonic vibration on dynamic recrystallization in friction stir welding," *Journal of Manufacturing Processes*, vol. 56, pp. 87–95, 2020.

[36] P. Pandita, V. P. Arya, G. Kaur, and S. Singh, "Particle size reduction of RDX by sequential application of solvent–antisolvent recrystallization and mechanical methods," *Journal of Energetic Materials*, vol. 38, no. 3, pp. 309–325, 2020.

[37] Z. Guo, M. Zhang, H. Li, J. Wang, and E. Kougoulos, "Effect of ultrasound on anti-solvent crystallization process," *Journal of Crystal Growth*, vol. 273, no. 3-4, pp. 555–563, 2005.

[38] H. Li, J. Wang, Y. Bao, Z. Guo, and M. Zhang, "Rapid sonocrystallization in the salting-out process," *Journal of Crystal Growth*, vol. 247, no. 1-2, pp. 192–198, 2003.

[39] Z. Ma, A. Pang, W. Li, Y. Qi, and L. Zhang, "Preparation and characterization of ultra-fine ammonium perchlorate crystals using a microfluidic system combined with ultrasonication," *Chemical Engineering Journal*, vol. 405, p. 126516, 2021.

[40] U. N. Hatkar and P. R. Gogate, "Process intensification of anti-solvent crystallization of salicylic acid using ultrasonic irradiations," *Chemical Engineering & Processing Process Intensification*, vol. 57-58, no. 1, pp. 16–24, 2012.

[41] J. Liu, J. Zhou, J. Zuo, K. Ye, and X. Jiang, "Experimental study on preparation of ultrafine explosive by air-jet grinding," *Aerospace Technology*, vol. 6, pp. 24–27, 2000.

[42] G. Deng and H. Liu, "Study on technology of making the superfine powder of RDX by grinding," *Explosive Materials*, vol. 38, no. 3, 2009.

[43] C. An, H. Li, and Y. Zhang, "Preparation and characterization of ultrafine HMX/TATB explosive co-crystals," *Central European Journal of Energetic Materials*, vol. 14, no. 4, pp. 876–887, 2017.

[44] L. J. Mccausland, P. W. Cains, and P. D. Martin, "Use the power of sonocrystallization for improved properties," *Chemical Engineering Progress*, vol. 97, no. 7, pp. 56–61, 2001.

[45] A. Abbas, M. Srour, P. Tang, H. Chiou, H. K. Chan, and J. A. Romagnoli, "Sonocrystallisation of sodium chloride particles for inhalation," *Chemical Engineering Science*, vol. 62, no. 9, pp. 2445–2453, 2007.

[46] X. Zhao, J. Rui, and S. Hong, "Recrystallization method for preparation of spherical RDX," *Transactions of Beijing Institute of Technology*, vol. 31, no. 1, pp. 5–7, 2011.

[47] X. Li, W. Yang, H. Liu, C. Song, H. Sun, and J. Tian, "Refined FOX-7 prepared by spray recrystallization method and the characterization of its performance," *Chinese Journal of Explosives & Propellants*, vol. 43, no. 6, pp. 662–668, 2020.

[48] S. Chin, J. Choi, H. Woo, J. H. Kim, H. S. Lee, and C. L. Lee, "Realizing a highly luminescent perovskite thin film by controlling the grain size and crystallinity through solvent vapour annealing," *Nanoscale*, vol. 11, no. 13, pp. 5861–5867, 2019.